Nonpolar resistive switching in Cu/SiC/Au non-volatile resistive memory devices

L. Zhong, L. Jiang, R. Huang, and C. H. de Groot

Citation: Applied Physics Letters **104**, 093507 (2014); doi: 10.1063/1.4867198
View online: http://dx.doi.org/10.1063/1.4867198
View Table of Contents: http://scitation.aip.org/content/aip/journal/apl/104/9?ver=pdfcov
Published by the AIP Publishing

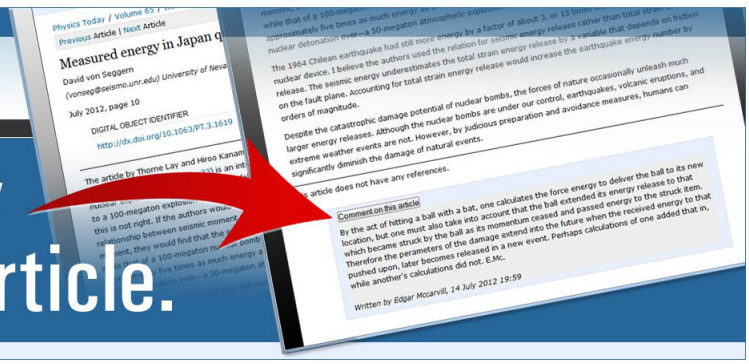

Nonpolar resistive switching in Cu/SiC/Au non-volatile resistive memory devices

L. Zhong,[1] L. Jiang,[1,a)] R. Huang,[2] and C. H. de Groot[2]
[1]*Faculty of Engineering and the Environment, University of Southampton, Southampton, Hampshire SO17 1BJ, United Kingdom*
[2]*Faculty of Physical Sciences and Engineering, University of Southampton, Southampton, Hampshire SO17 1BJ, United Kingdom*

(Received 4 December 2013; accepted 13 February 2014; published online 4 March 2014)

Amorphous silicon carbide (a-SiC) based resistive memory (RM) Cu/a-SiC/Au devices were fabricated and their resistive switching characteristics investigated. All four possible modes of nonpolar resistive switching were achieved with ON/OFF ratio in the range 10^6–10^8. Detailed current-voltage I-V characteristics analysis suggests that the conduction mechanism in low resistance state is due to the formation of metallic filaments. Schottky emission is proven to be the dominant conduction mechanism in high resistance state which results from the Schottky contacts between the metal electrodes and SiC. ON/OFF ratios exceeding 10^7 over 10 years were also predicted from state retention characterizations. These results suggest promising application potentials for Cu/a-SiC/Au RMs. © *2014 AIP Publishing LLC*. [http://dx.doi.org/10.1063/1.4867198]

Conventional Si charge-storage-based non-volatile memories are running into serious limitations as further down-scaling leads to difficulties in retaining reliable performance.[1] In recent years, this dilemma has triggered great interest and development of resistance random access memory for next generation non-volatile memory due to its promising performance and potentials including down-scalability, excellent endurance, simple structures, fast speed, low power consumption, and back-end of line compatibility.[2] A resistive memory (RM) usually consists of an insulating or semiconducting material which is sandwiched between two metal electrodes. Reversible resistive switching is modulated by applying a voltage across the metal electrodes to achieve the transition from high (HRS) to low (LRS) resistance state (SET) or the transition from LRS to HRS (RESET). Resistance of device at LRS and HRS are often noted as R_{ON} and R_{OFF}, respectively.

A number of RMs has been reported with resistive switching behaviour. Based on current-voltage (I-V) characteristics, the switching modes can be classified into three main types: unipolar, bipolar, and nonpolar. Unipolar resistive memories refer to RMs which can be SET and RESET by applying voltages with the same polarity, while bipolar RMs require opposite voltage polarities to SET and RESET for each switching cycle. A typical bipolar RM usually contains two different electrodes as one is electrochemically active and the other is inert.[2] This is to enable the voltage polarity dependant filamentary formation during SET and rupture during RESET based on electrochemical reaction in the middle solid electrolyte layer.[3,4] On the other hand, the same metal is generally used for both electrodes in a typical unipolar RM to enable SET/RESET under the same voltage polarity.[5,6] Relatively speaking, bipolar switching features faster switching speed, better uniformity, and lower operation power,[7] while unipolar switching presents higher ON/OFF ratios (R_{OFF}/R_{ON}) and presents advantages for high density integration.[8] Thus nonpolar RMs which exhibit both unipolar and bipolar switching behaviours have been considered advantageous as they can potentially expand application scopes of RMs.[9] It is worth noting that there can be two possible bipolar switching modes in one device which can be defined as positive bipolar achieved by positive SET voltage (V_{SET}) followed by negative RESET voltage (V_{RESET}) and negative bipolar achieved by negative V_{SET} followed by positive V_{RESET}. Similarly two possible unipolar switching modes can exist in one device which can be defined as positive unipolar (positive V_{SET} followed by positive V_{RESET}) and negative unipolar (negative V_{SET} followed by negative V_{RESET}). Nonpolar devices ideally should present all these four possible switching modes.

Only a limited number of nonpolar RMs have been reported to present all four possible switching modes. Most of them are transition metal oxide based RMs[4,5] or insulating material based RMs with metal dopants or particles embedded in the switching layers.[6,8] However, introduction of dopants into the switching layers can reduce the resistance in HRS, leading to limited ON/OFF ratios.[10] Furthermore, despite of different device configurations, most reported nonpolar RMs are attributable to the same conductive filaments when subject to positive V_{SET} or negative V_{SET}, hence similar resistant states, i.e., R_{ON}, R_{OFF}, and switching ratios were observed.[5,8] For example, positive bipolar and negative bipolar switching performance can be similar or symmetric.[6] If the change of polarity could also induce asymmetric switching performance such as R_{ON}, R_{OFF}, and switching ratios, this may be further exploited to expand the potential programmable range of future RMs.

Amorphous silicon carbide (a-SiC) based RMs has recently been reported to show very promising resistive switching behaviours.[3,11] Our previous results also suggest that ultrahigh switching ratios in the range of 10^8–10^9 can be achieved.[12] In this paper, we report a-SiC based RMs which exhibit nonpolar switching characteristics, high ON/OFF ratios, and excellent retention performance. Asymmetric bipolar and unipolar switching behaviours are investigated based

a)Email: L.Jiang@soton.ac.uk

on the formation and rupture of conductive filaments in all four switching modes.

Cu/a-SiC/Au RM cells were fabricated on Si wafers covered with a 1 μm thick thermal SiO_2 layer. 300 nm Au was deposited by magnetron sputtering followed by the deposition of a 250 nm thick SiO_2 layer. Photolithography and reactive ion etching were then conducted to pattern and expose the active device areas. Subsequently, 40 nm thick a-SiC and 300 nm thick Cu layers were deposited without breaking the sputtering chamber vacuum on the patterned substrates. A final lift off process was used to achieve the Cu/a-SiC/Au RM devices. All processes were conducted at room temperature. I-V characteristics were measured by voltage sweeps using an Agilent B1500A semiconductor device parameter analyser. All voltage sweeps were conducted by grounding the Au electrode while applying polarized voltages on the Cu electrode. A current compliance of 100 μA was applied for all SET switching process, and no compliance current was applied during RESET. A cross-section view of a typical device and the schematic of voltage application are shown in the inset of Figure 1(d).

Material composition of the as-deposited a-SiC has been characterised by X-ray photoelectron spectroscopy (XPS). Figures 1(a) and 1(b) show that Si 2p and C 1s peaks are at 100.7 eV and 283.3 eV, respectively, which corresponds to stoichiometric a-SiC.[13] High resolution X-ray diffraction (XRD) spectra have been obtained from both the SiC sputtering target as well as as-deposited SiC layer, as shown in Figure 1(c). The characteristic 3C-SiC (111) XRD peak at 35.7° (Ref. 14) is clearly observed from the SiC target, while no peaks are shown from the as-deposited SiC layer, suggesting amorphous status of the as-deposited SiC. Furthermore, by analysing the capacitance of pristine Cu/a-SiC/Au devices with varied device areas, as shown in Figure 1(d), dielectric constant ε and refractive index n of the a-SiC layer can also been estimated to be 6.5 and 2.55, respectively, which also corresponds to C/Si ratio of 1.[15]

To avoid any possible influence from switching history, in this work, each of the four switching mode i.e., positive bipolar (+bipolar), negative bipolar (−bipolar), positive unipolar (+unipolar), negative unipolar (−unipolar) was conducted using a pristine Cu/a-SiC/Au device with identical device structures, i.e., each device has only been tested using its respective switching mode. In order to ensure the uniformity of the device performance, at least five identical devices have been measured for each switching mode, and for each switching device, at least 20 cycles have been conducted. All four switching characteristics have been observed over a range of devices, respectively, which have also shown reliability over repeated switching cycles (not shown here). As the starting state of pristine Cu/a-SiC/Au RMs is always HRS, a first electroforming process is observed for all these switching mode to obtain the initial LRS with the forming voltage in the range of 4–5 V, as shown in Figures 2(a) and 2(b). Higher forming voltage for a pristine device as in contrast to V_{SET} in the subsequent SET and RESET cycles has been frequently observed in many RMs, which is attributed to the requirement to induce the

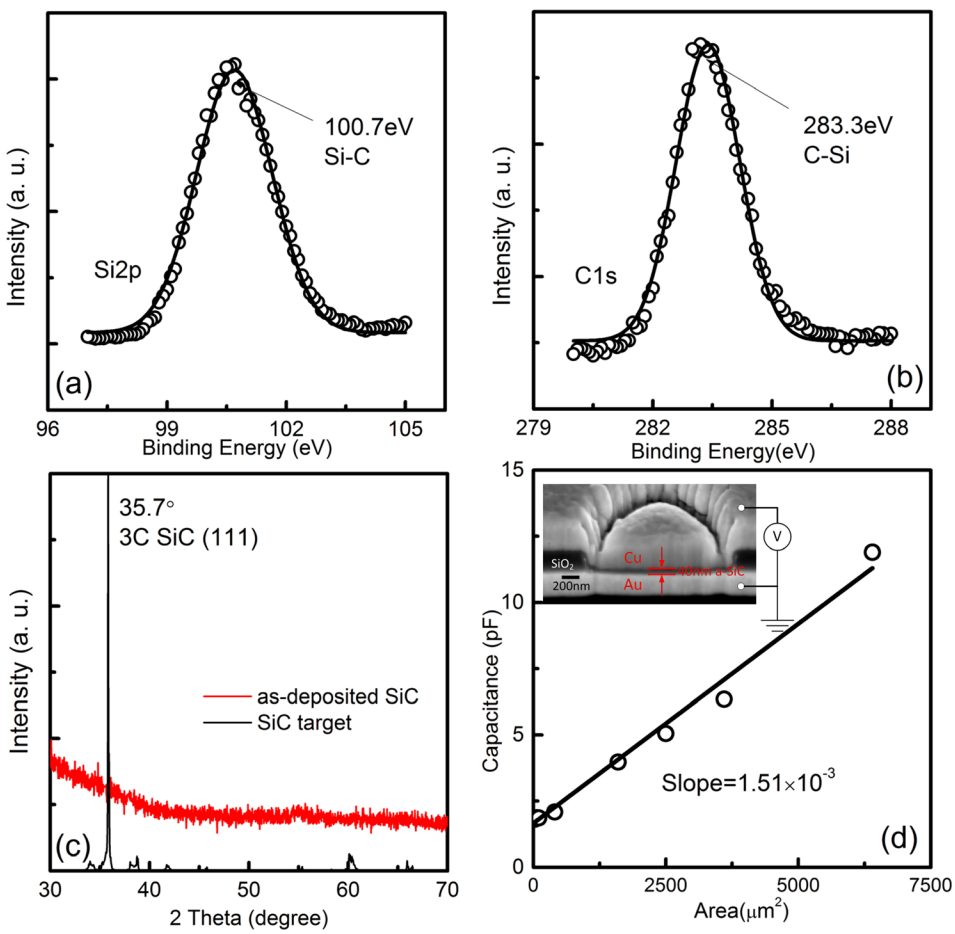

FIG. 1. (a) Si 2p and (b) C 1s XPS spectra of as-deposited a-SiC film, with peak binding energy labelled. (c) XRD spectra of SiC sputtering target and as-deposited a-SiC film. (d) Capacitance of pristine Cu/a-SiC/Au devices with varied device area. The inset shows the cross-section of a typical device with a schematic indication of electric connection configuration for the switching tests.

conductive paths through the entire thickness of the device layer.[16] Typical I-V characteristics of the stable switching cycles of the Cu/a-SiC/Au devices with 1 μm^2 device area are also shown in Figures 2(c) and 2(d), presenting all four unipolar switching modes, respectively. It is observed that typical V_{SET} and V_{RESET} are around or below 2 V. It is worth noting that, high switching ratios in the range of 10^6–10^8 were obtained for all four modes. Asymmetric switching performances between positive bipolar and negative bipolar cycles as well as between positive unipolar and negative unipolar cycles are observed. For instance, switching ratios for negative bipolar and negative unipolar are approximately two orders of magnitude higher than positive bipolar and positive unipolar modes, respectively.

To investigate the switching mechanisms, detailed I-V characteristics for LRS and HRS are plotted in Figure 3. Straight lines with slope of approximately unity are obtained for all LRS in a double logarithmic plot (Figure 3(a)), which indicates Ohmic conduction, most likely due to filamentary conduction.[2] It is believed that, when the device is subject to an applied electrical field during SET process, conductive filaments are formed by redox reaction of the electrochemically active metal electrode followed by ion migration and deposition within the insulating layer. For the herein reported Cu/a-SiC/Au devices, when positive voltage is applied to the Cu electrode, i.e., SET processes for positive bipolar and positive unipolar modes, Cu atoms are oxidized to Cu^{z+} ions which migrate through the a-SiC layer and subsequently reduce to Cu atoms at the Au counter electrode and eventually form Cu filaments. Cu as an electrochemically active material has been widely used in many RMs[2–4,11] with real time observation of Cu filaments observed using high resolution transmission electron microscopy (TEM).[17] In comparison with Cu, Au has a much higher reduction potential[18] and thus has mainly been used as inert counter electrodes in RMs.[19] Nevertheless, real time TEM observation of Au filaments has been recently reported.[20] For our Cu/a-SiC/Au devices, when negative voltage is applied to the Cu electrode during SET process, i.e., negative bipolar and negative unipolar modes, the Au electrode is subject to a positive electrical field where, we believe, Au atoms can be oxidized to Au^+ ions which reduce to Au atoms at the Cu counter electrode and thus form Au conductive filaments. To further clarify these conduction mechanisms, Figure 4 shows R_{ON} as a function of temperature. As expected, metallic behaviour is observed for the LRS resistance for both positive (R_{ON+}) and negative (R_{ON-}) switching modes. Through linear fitting, the temperature coefficient of R_{ON+} and R_{ON-} are extracted to be 2.4×10^{-3} K^{-1} and 2.7×10^{-3} K^{-1}. These values are in agreement with reported values for Cu nanowires (2.5×10^{-3} K^{-1})[21] and Au nanowires (2.3×10^{-3} K^{-1}),[22] respectively. These results also discard the possibility of any oxygen vacancy conduction

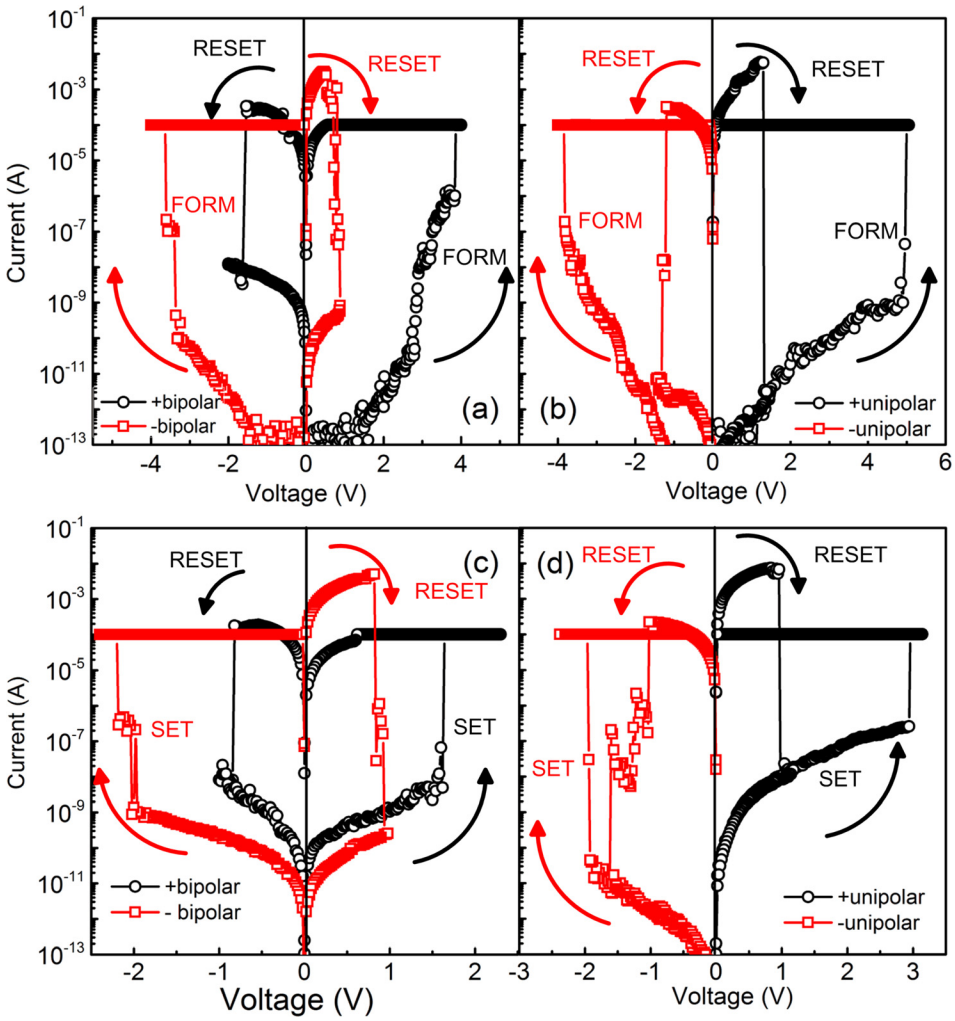

FIG. 2. I-V curves of electroforming cycles and typical switching cycles of all four possible switching modes: (a) electroforming cycles of +bipolar and −bipolar modes, (b) electroforming cycles of +unipolar and −unipolar modes, (c) typical switching cycles of +bipolar and −bipolar modes, (d) typical switching cycles of +unipolar and −unipolar modes. The arrows indicate the respective voltage sweeping directions.

as its temperature coefficient should be at least an order of magnitude smaller than metal filaments.[23]

Figure 3(b) shows the HRS I-V characteristics of all the four switching modes which can be explained by Schottky Emission mechanism following:[24]

$$I = AA^*T^2 \exp\left[\frac{-q\Phi_B}{kT} + \frac{q\sqrt{q/4\pi\varepsilon_i}}{kT}\sqrt{E}\right], \qquad (1)$$

where A is the conduction area, A^* is Richardson's constant, Φ_B is Schottky Barrier Height (SBH), E is electrical field, q is the electronic charge, k is the Boltzmann's constant, ε_i is dielectric constant of the film, and T is absolute temperature. This is expected as SiC have been widely exploited for Schottky diode applications.[25] The existence of Schottky contacts between the metal electrodes and a-SiC in this case is advantageous for Cu/a-SiC/Au RMs as it contributes to the high R_{OFF}, leading to high switching ratios. Furthermore, it is observed that the R_{OFF} values for negative bipolar and negative unipolar modes are over an order of magnitude higher than positive bipolar and positive unipolar modes, respectively. This is probably due to the higher work function of Au nanowires in the negative bipolar and negative unipolar modes in comparison with Cu nanowires in positive bipolar and positive unipolar modes, which leads to higher

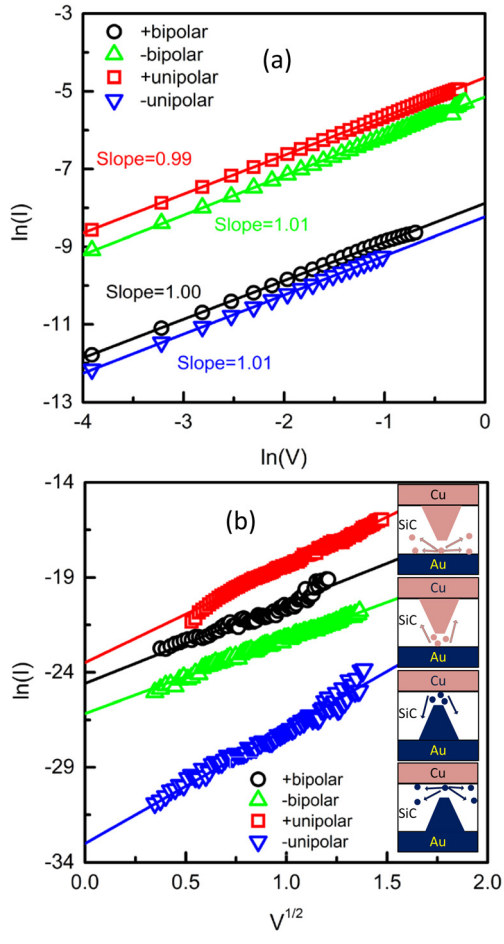

FIG. 3. (a) LRS I-V data in Ln(I)-Ln(V) plots, with respective linear fittings. (b) HRS I-V data in Ln(I)-$V^{1/2}$ plots, with linear fittings to the Schottky emission equation. The insets illustrate the possible RESET mechanisms for each switching mode: +unipolar, +bipolar, −bipolar, and −unipolar in top-down sequence.

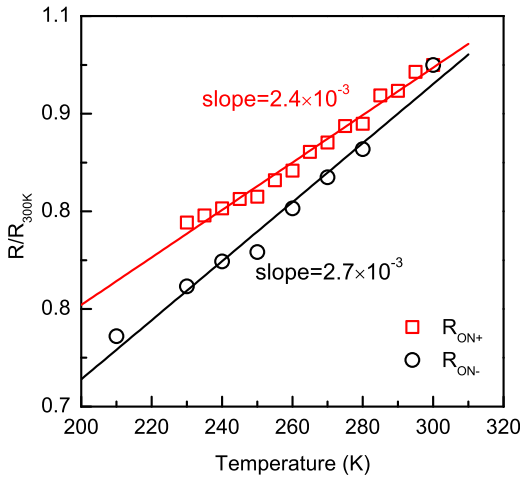

FIG. 4. Normalized R_{ON} values versus temperature, with the straight lines being their respective linear fittings.

Φ_B when in contact with a-SiC in HRS. Rupture of the conductive filaments has been reported to underpin the RESET process. We believe that in our Cu/a-SiC/Au devices, electrochemical dissolution of the metal filaments plays the dominant role in bipolar switching,[2] while Joule heating enhanced lateral diffusion dominates RESET in unipolar switches. The fact that our devices have clearly demonstrated stable resistive switching when Cu and Au electrodes are subjected to positive electrical fields suggest that the Au electrode is not only inert enough to enable positive bipolar and positive unipolar switching cycles but also active enough to allow negative bipolar and negative unipolar switching behaviours. Furthermore, both Cu and Au have very low diffusion coefficients in SiC,[26,27] suggesting Cu or Au ions are apt to be reduced before they reach their respective counter electrode and thus result in a cone-shaped filament with the narrowest point near the counter electrode.[15,28] We thus believe that the rupture of the filaments for Cu/a-SiC/Au RMs is likely to occur at this narrowest point, as insets in Figure 3(b) illustrate the possible RESET mechanisms for each switching mode.

Figure 5 shows the retention performance of R_{ON} and R_{OFF} states. There is no noticeable deterioration over the

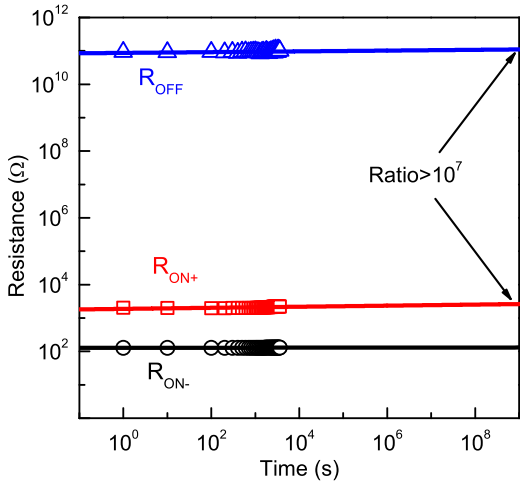

FIG. 5. R_{ON} and R_{OFF} values versus time measured at 85 °C, with power law extrapolation to 10 years.

measurement duration at 85 °C. The power-law extrapolation[29] suggests that the ON/OFF switching ratio after 10 years can still be expected to be greater than 10^7, implying excellent stability and retention of these devices. This might be attributable to the high chemical stability of SiC material as well as the low Cu and Au diffusion in SiC.[26,27] As a result, these a-SiC based RMs using Cu and Au electrodes demonstrate significant advantages and potential for future applications.

In summary, Cu/a-SiC/Au devices with nonpolar resistive switching characteristics are obtained and analysed. All four possible switching modes are present with asymmetric switching performance, such as R_{ON}, R_{OFF}, and switching ratio between positive bipolar and negative bipolar modes as well as between positive unipolar and negative unipolar modes. Detailed I-V characteristics analysis suggests that the conduction mechanism in LRS is due to the formation of Cu or Au filaments. Schottky emission is proven to be the dominant conduction mechanism in HRS, which results from the Schottky contacts between the metal electrodes and SiC. The rupture of the filaments in the RESET process is likely to be attributable to electrochemical dissolution for bipolar modes and Joule heating assistant diffusion for unipolar modes. The combination of Cu and Au as electrodes in the a-SiC RM has proven to be effective in enabling all four possible nonpolar switching modes. The Cu/a-SiC/Au devices also show excellent retention performance. These results suggest promising application potentials for Cu/a-SiC/Au RMs.

[1]B. C. Lee, Z. Ping, Y. Jun, Z. Youtao, Z. Bo, E. Ipek, O. Mutlu, and D. Burger, IEEE Micro **30**, 143 (2010).
[2]R. Waser, R. Dittmann, G. Staikov, and K. Szot, Adv. Mater. **21**, 2632 (2009).
[3]W. Lee, J. Park, M. Son, J. Lee, S. Jung, S. Kim, S. Park, J. Shin, and H. Hwang, IEEE Electron Device Lett. **32**, 680 (2011).
[4]K. L. Lin, T. H. Hou, J. Shieh, J. H. Lin, C. T. Chou, and Y. J. Lee, J. Appl. Phys. **109**, 084104 (2011).
[5]H.-H. Huang, W.-C. Shih, and C.-H. Lai, Appl. Phys. Lett. **96**, 193505 (2010).
[6]C. Chao, G. Shuang, T. Guangsheng, S. Cheng, Z. Fei, and P. Feng, IEEE Electron Device Lett. **33**, 1711 (2012).
[7]L. Goux, J. G. Lisoni, M. Jurczak, D. J. Wouters, L. Courtade, and C. Muller, J. Appl. Phys. **107**, 024512 (2010).
[8]M. C. Wu, T. H. Wu, and T. Y. Tseng, J. Appl. Phys. **111**, 014505 (2012).
[9]J.-S. Huang, L. M. Chen, T. Y. Lin, C. Y. Lee, and T. S. Chin, Thin Solid Films **544**, 134 (2013).
[10]S. J. Choi, K. H. Kim, G. S. Park, H. J. Bae, W. Y. Yang, and S. Cho, IEEE Electron Device Lett. **32**, 375 (2011).
[11]W. Lee, M. Siddik, S. Jung, J. Park, S. Kim, J. Shin, J. Lee, S. Park, M. Son, and H. Hwang, IEEE Electron Device Lett. **32**, 1573 (2011).
[12]L. Zhong, P. A. Reed, R. Huang, C. H. de Groot, and L. Jiang, "Amorphous SiC based non-volatile resistive memories with ultrahigh ON/OFF ratios" Microelectron. Eng. (to be published).
[13]W. C. Mohr, C. C. Tsai, and R. A. Street, MRS Online Proc. Lib. **70**, 319 (1986).
[14]A. Gupta, D. Paramanik, S. Varma, and C. Jacob, Bull. Mater. Sci. **27**, 445 (2004).
[15]S. Janz, Ph.D thesis, "Amorphous Silicon Carbide for Photovoltaic Applications," Universität Konstanz, Fakultät für Physik, 2006; available online at http://d-nb.info/98503534X/34.
[16]J. J. Yang, D. B. Strukov, and D. R. Stewart, Nat. Nanotechnol. **8**, 13 (2013).
[17]Q. Liu, J. Sun, H. Lv, S. Long, K. Yin, N. Wan, Y. Li, L. Sun, and M. Liu, Adv. Mater. **24**, 1844 (2012).
[18]A. J. Bard, R. Parsons, and J. Jordan, *Standard Potentials in Aqueous Solution* (Marcel Dekker, New York, 1985).
[19]Y. Bernard, P. Gonon, and V. Jousseaume, Appl. Phys. Lett. **96**, 193502 (2010).
[20]C. N. Peng, C. W. Wang, T. C. Chan, W. Y. Chang, Y. C. Wang, H. W. Tsai, W. W. Wu, L. J. Chen, and Y. L. Chueh, Nanoscale Res. Lett. **7**, 559 (2012).
[21]A. Bid, A. Bora, and A. K. Raychaudhuri, Phys. Rev. B **74**, 035426 (2006).
[22]S. Karim, W. Ensinger, T. W. Cornelius, and R. Neumann, Physica E **40**, 3173 (2008).
[23]Z. Q. Wang, H. Y. Xu, L. Zhang, X. H. Li, J. G. Ma, X. T. Zhang, and Y. C. Liu, Nanoscale **5**, 4490 (2013).
[24]S. M. Sze, *Physics of Semiconductor Devices*, 2nd ed. (John Wiley & Sons, New York, 1981).
[25]L. M. Porter and R. F. Davis, Mater. Sci. Eng. B **34**, 83 (1995).
[26]N. Kornilios, G. Constantinidis, M. Kayiambaki, K. Zekentes, and J. Stoemenos, Mater. Sci. Eng. B **46**, 186 (1997).
[27]A. Suino, Y. Yamazaki, H. Nitta, K. Miura, H. Seto, R. Kanno, Y. Iijima, H. Sato, S. Takeda, E. Toya *et al.*, J. Phys. Chem. Solids **69**, 311 (2008).
[28]S. Peng, F. Zhuge, X. Chen, X. Zhu, B. Hu, L. Pan, B. Chen, and R. W. Li, Appl. Phys. Lett. **100**, 072101 (2012).
[29]I. Valov, R. Waser, J. R. Jameson, and M. N. Kozicki, Nanotechnology **22**, 254003 (2011).